

Supplementary Information

Impact of Nitrogen Configuration on the Electronic Properties of Tailored Triphenylamine Derivatives as Hole Transport Materials for Perovskite Solar Cells: A Computational Chemistry Study

Raul Flores, Nora Aydeé Sánchez-Bojorge, Juan Pedro Palomares-Báez, Linda-Lucila Landeros-Martínez and Luz María Rodríguez-Valdez**

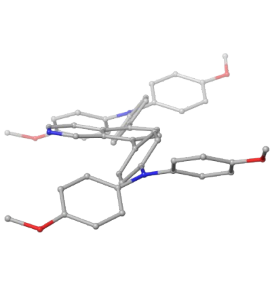
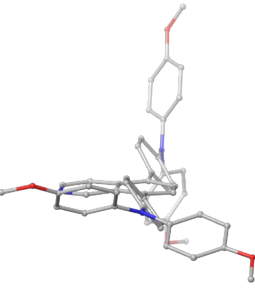
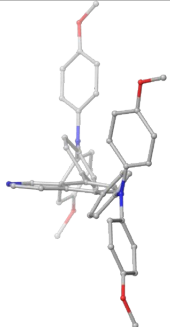
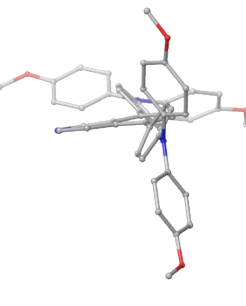
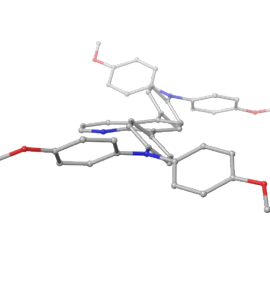
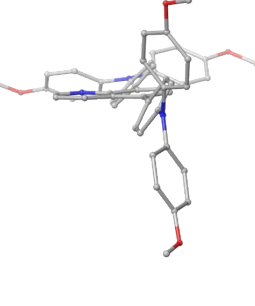
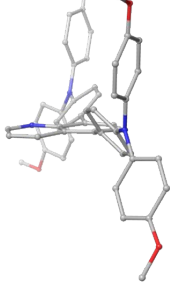
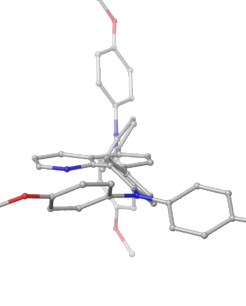
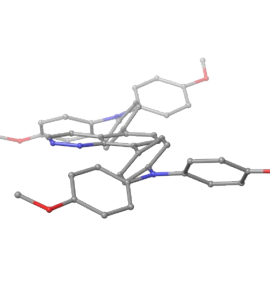
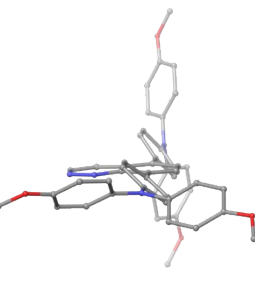
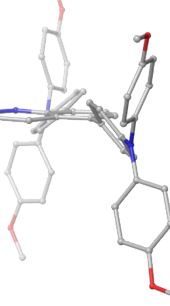
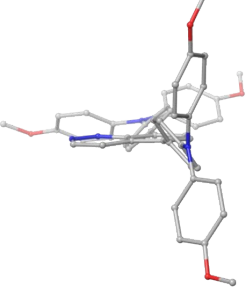
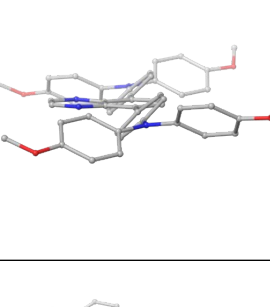
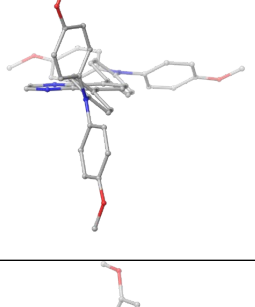
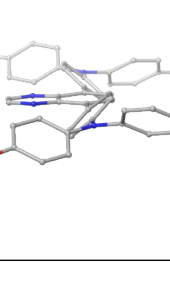
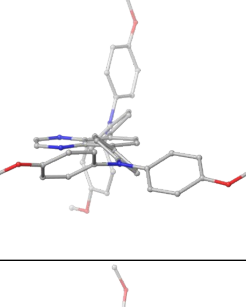
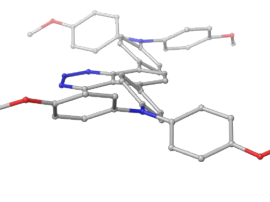
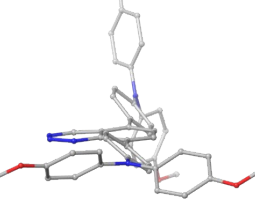
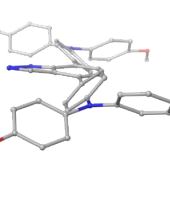
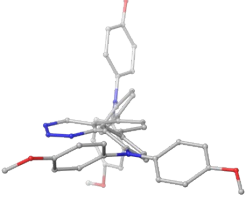
Laboratorio de Química Computacional, Facultad de Ciencias Químicas, Universidad Autónoma de Chihuahua, Circuito Universitario S/N, Campus UACH II, Chihuahua, Chihuahua, C.P. 31125, México; E-mail: lmrodrig@uach.mx, ppalomares@uach.mx

Table SI 1. Electronic couplings of n-TPAM dimers calculated with ω -opt-B97X-3c/6-311G(d,p) and ω -opt-B97X-3c/vDZP. Reorganisation energies of n-TPAM, YZ22, and YZ18 molecules located with CREST. The complete DFT-CP methods deposited on Zenodo at <https://doi.org/10.5281/zenodo.11391494>

π -linker	conformer	$J_{\text{eff}}(\text{h})$ meV		<i>se</i>	<i>ss</i>
		ω B97X-3c	ω 6-311G(d,p)		
A	1	144.13	142.95		
	2	124.47	123.42		
	3	109.25	108.12		
	4	38.21	37.69		
	5	22.74	22.79		
B	1	157.24	155.57		
	2	150.38	148.64		
	3	109.68	108.96		
	4	107.73	107.43		
	5	39.55	34.06		
C	2	147.39	146.33		
	1	145.17	144.26		
	3	123.95	123.02		
	4	4.53	4.82		
D	1	161.38	159.98		
	2	161.35	158.88		
	3	45.04	45.98		
	4	16.04	16.98		
E	2	155.12	153.98		
	1	148.99	147.88		
	3	112.71	110.80		
	4	43.34	43.59		
F	2	161.55	160.41		
	1	159.30	158.27		
	3	39.58	39.90		

Table SI 2. Reorganisation energies of n-TPAM, YZ22, and YZ18 calculated with ω -opt-B97X-3c/vDZP, ω -opt-B97X-3c/6-311G(d,p) and M06/6-311G(d,p)

	ω -opt-B97X-3c		M06
	vDZP	6-311G(d,p)	6-311G(d,p)
A-TPAM	346.31	320.60	189.92
B-TPAM	268.76	271.03	191.70
C-TPAM	283.34	279.53	183.05
D-TPAM	321.84	311.21	185.83
E-TPAM	304.07	302.56	174.66
F-TPAM	291.25	302.54	161.32
YZ22	149.78	148.91	128.20
YZ18	187.81	179.51	133.80

A-TPAM				
B-TPAM				
C-TPAM				
D-TPAM				
E-TPAM				

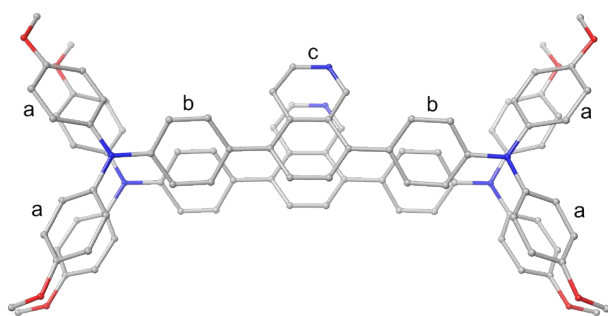
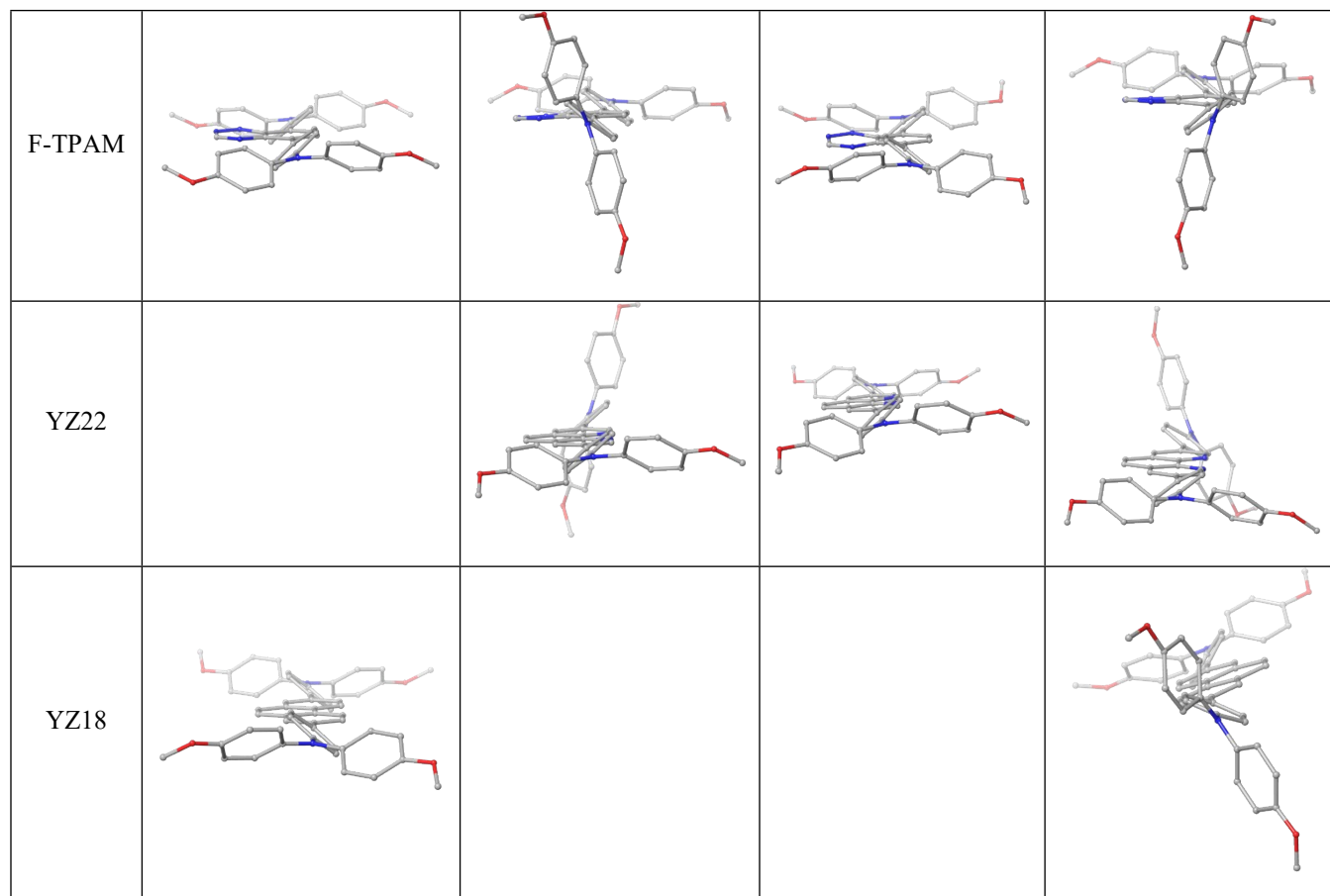


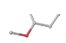
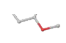
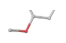
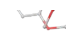








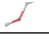
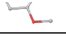


Figure SI 1. Labelling of π - π stacked rings of n-TPAM, YZ18, and YZ22 dimers.











Table SI 4. Average distance between ring centres (R_c) of π - π stacked rings obtained from geometry optimisation at the dftb3-3ob-MBD level of theory; a, b, and c correspond to the Figure SI 1 labelling.

conformer	a	b	c
-----------	---	---	---



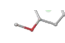

A-TPAM	1	4.25	4.00	3.93		
	2	4.26	4.07	4.11		
	3	4.18	4.49	4.71		
	4	4.19	4.15	4.38		
	5	3.94		3.60		
B-TPAM	1	4.22	3.96	3.74		
	2	4.22	4.00	4.04		
	3	4.27	4.16	3.86		
	4	4.23	3.96	3.70		

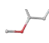





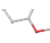










						
	5	4.18	4.22	3.87		
						

C-TPAM

	1	4.27	3.93	3.72		
						
	2	4.28	3.95	3.96		
						
	3	4.41	4.04	3.64		
						
						
	4			3.51		
						

D-TPAM

	1	4.22	3.92	3.61		
						
	2	4.26	3.88	3.91		
						
	3					

							
	4						
	<hr/>						
	1	4.24	3.97	3.72			
	2	4.26	3.90	3.59			
E-TPAM	3	4.20	4.02	3.83			
	4	4.15	4.11	4.03			
	1	4.21	3.94	3.58			
F-TPAM	2	4.21	4.30	3.90			
	<hr/>						
	3						
	<hr/>						

Average	4.22	4.05	3.86
---------	------	------	------

Table SI 5. Geometrical characteristics of YZ18, YZ22, and n-TPAM dimers calculated with r2scan-3c/def2-mTZVPP geometry optimisations.

cnf		R_c		θ_a	
		r2scan-3c	Dftb3-MBD	r2scan-3c	Dftb3-MBD
A	s	4.40	4.18	21.0	4.6
	e	4.30	4.10	28.9	3.8
B	s	4.32	4.12	25.6	3.8
	e	4.23	4.04	24.7	4.4
C	s	4.43	4.12	25.6	4.1
	e	4.39	4.05	26.3	3.3
D	s	4.26	4.08	21.7	3.2
	e	4.21	3.99	18.1	3.9
E	s	4.38	4.21	26.5	4.8
	e	4.23	4.04	26.2	4.0
F	s	4.33	4.16	27.2	4.1
	e	4.19	3.99	23.0	4.3
YZ22	s	4.22	4.01	24.1	3.8
	e	4.31	3.97	19.8	3.3
YZ18	e	4.26	3.98	22.5	3.8
	s	4.24	4.00	22.5	4.4

^aAverage angle between the planes of the π - π stacked rings of end-cap TPAM

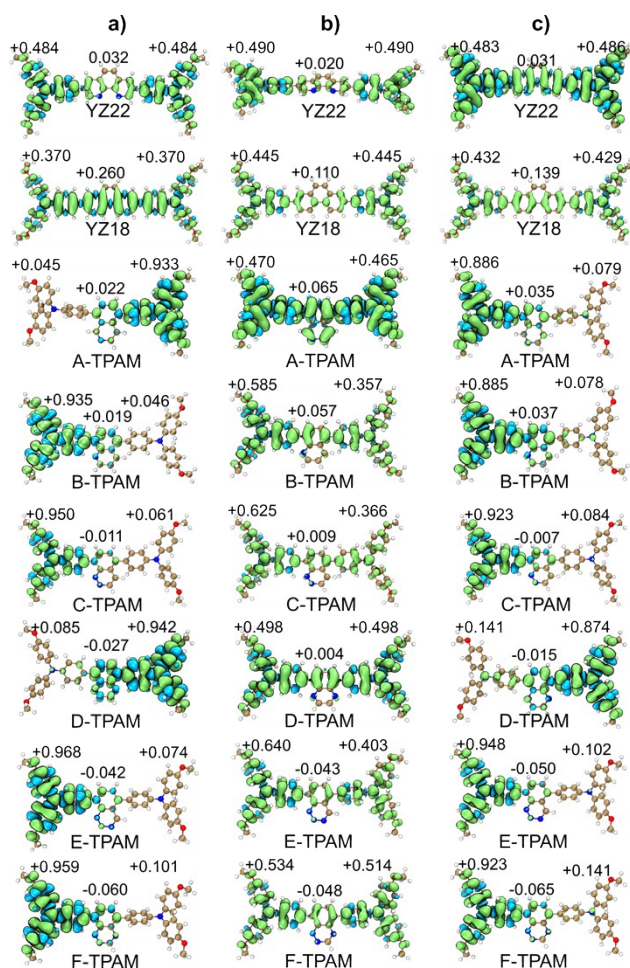


Figure SI 2 Contour plots of electron spin densities and MBIS fragment charge populations of cation n-TPAM, YZ22, and YZ18. The numbers on the left and right of each contour plot indicate the TPAM fragment charge, and the number in the middle is the core charge. a) ω B97X-3c/vDZP b) M06/6-311G(d,p) c) ω -opt-B97X-3c/vDZP

Table SI 6. Wavelength of the lowest energy excitation (λ_{\max}), oscillator strength, and the HOMO(H0)-LUMO(L0) transitions of n-TPAM, YZ22, and YZ18 calculated with ω -opt-B97X-3c/vDZP

	λ_{\max} (nm)	Oscillator strength(f)	H0 \rightarrow L0 electronic transitions (%)
A-TPAM	331.4	1.2221	67.3
B-TPAM	349.9	0.9950	72.2
C-TPAM	412.1	0.1160	19.3
D-TPAM	385.7	0.6913	78.9
E-TPAM	394.3	0.7514	75.2
F-TPAM	470.6	0.0398	6.7
YZ18	329.6	2.4885	62.1
YZ22	336.2	2.3432	64.0

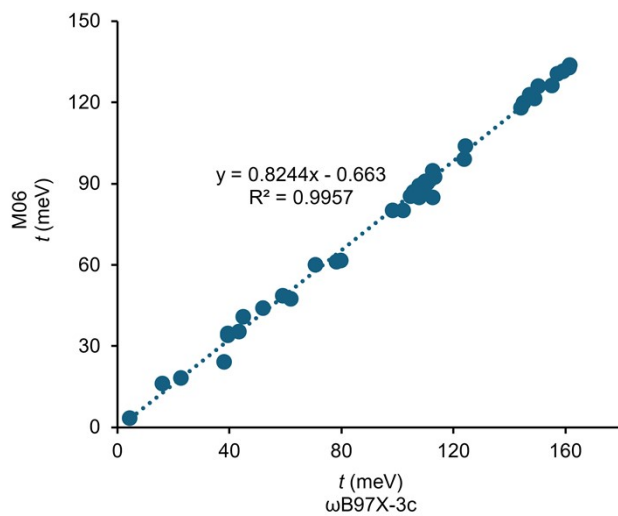


Figure SI 3 Scatter plot of the correlation coefficient ($R^2 = 0.9957$) between the charge transfer integral (t) computed with ω B97X-3c/vDZP and M06/6-311G(d,p) functionals using the DIPRO method.

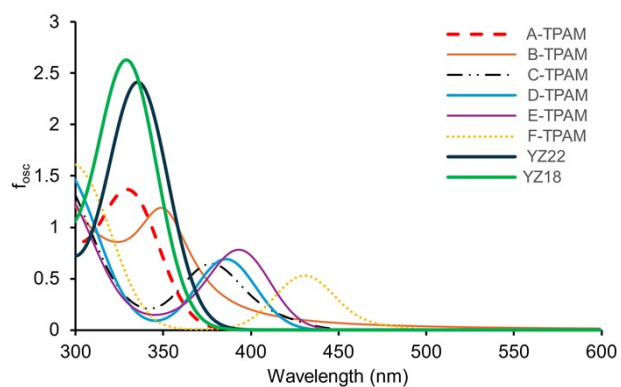


Figure SI 4 UV-Vis absorption spectrum of n-TPAM, YZ22, and YZ18 molecules computed using 40 roots with TD-DFT ω -opt-B97X-3c/vDZP.